On the stability of a falling liquid curtain

Peter J. Schmid, D.S. Henningson

J. Fluid Mech. (2002), *vol.* 463, *pp.* 163–171.
DOI: 10.1017/S002211200200873X Printed in the United Kingdom

On the stability of a falling liquid curtain

By PETER J. SCHMID[1]† AND DAN S. HENNINGSON[2]

[1]Laboratoire d'Hydrodynamique (LadHyX), École Polytechnique, F-91128 Palaiseau, France
[2]Department of Mechanics, Royal Institute of Technology, S-10044 Stockholm, Sweden

(Received 8 February 2002 and in revised form 20 March 2002)

The stability of a falling liquid curtain is investigated. The sheet of liquid is assumed two-dimensional, driven by gravity and influenced by a compressible cushion of air enclosed on one side of the curtain. The linear stability problem is formulated in the form of an integro-differential eigenvalue problem. Although experimental efforts have consistently reported a peak in the low-frequency range of the spectrum, the linear stability results do not show instabilities at these frequencies. However, a multi-modal approach combined with a projection onto low-frequency modes reveals a dominant and robust instability feature that is in good agreement with experimental measurements. This instability manifests itself as a wave packet, consisting of a linear superposition of linear global modes, that travels down the curtain and causes a strong pressure signal in the enclosed air cushion.

1. Introduction

It is well known that thin water curtains that enclose a volume of air on one side (see figure 1) can exhibit self-sustained oscillations which can lead to significant noise levels and/or structural damage (see e.g. Schwartz 1966; Cremer & Ising 1972; Casperson 1993). This is easily verified by observing the flow of waterfalls, dams or weirs. The frequency of these oscillations is selected based on a coupling of an instability in the fluid system to a feedback mechanism due to the pressure variations in the air pocket (Naudascher & Rockwell 1994). Horizontal motions of the liquid curtain lead to pressure variations in the air pocket which, in turn, modify the deflection of the curtain. This feedback mechanism is strongest in closed air pockets, even though it can also be observed in aerated air pockets (Falvey 1980).

Fluid oscillators enclosing a volume of gas have previously been studied, the simplest examples being a spherical gas bubble in a liquid or a pulsating cavitation bubble behind obstacles (e.g. Plesset & Prosperetti 1977). Little attention, however, has been paid to liquid sheets whose oscillatory behaviour is modified by pressure variations in the gas volume that they create. Most of the results on water curtain oscillations have been of an experimental nature (e.g. Carman 1960; Kemp & Pullen 1961; Partenscky & Khloeung 1967) and report the selection of a distinct time scale close to an integer multiple of the fall time of a particle within the sheet. Among the few theoretical efforts to explain this frequency selection, Treiber (1974) argued that a resonance condition between the pressure oscillations in the air cushion and the pressure variations caused by the oscillating curtain is responsible for the experimentally observed frequency. Assuming sinusoidal pressure variations in the air

† Permanent address: Department of Applied Mathematics, University of Washington, Seattle, WA 98195-2420, USA.

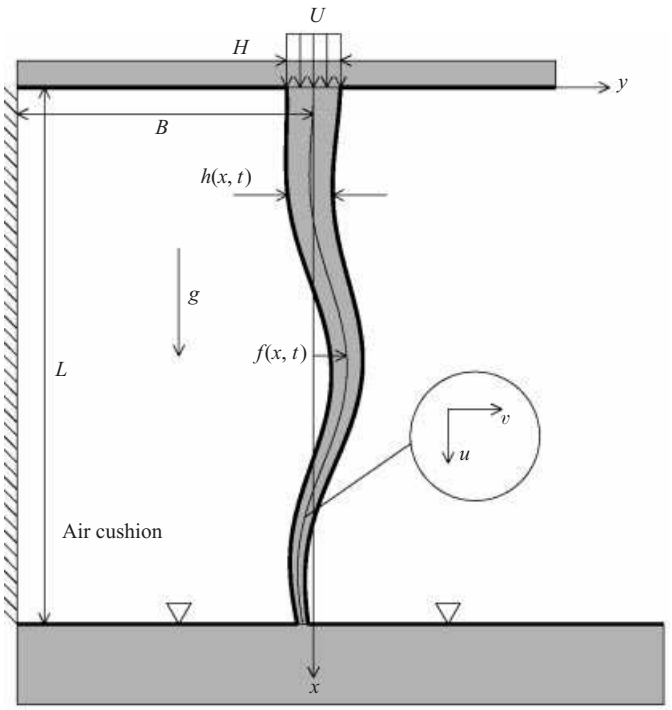

FIGURE 1. Sketch of the geometry for a falling liquid sheet.

pocket and modelling the flow in the curtain by a Lagrangian description of the path of fluid particles under gravity only, he arrived at a frequency selection condition that matched experimental results.

In this paper, we revisit the problem of liquid curtain oscillations influenced by an enclosed compressible air cushion, but treat it as an instability of a globally coupled system rather than as a resonant dynamical system. No *a priori* assumptions about the time-dependence of the pressure oscillations or the shape of the liquid sheet are made. An Eulerian framework is used to formulate the governing equations of motion and a linear stability analysis based on low-frequency modes is presented. Experimental data by L.-G. Sundström, L. Fäldt & F. Bark (1993, personal communication) and Baille (1994) will be used to verify our results.

2. Mathematical description

The derivation of the governing equations for an oscillating liquid curtain follows the standard procedure of formulating mass and momentum balances on an infinitesimal control volume. Figure 1 shows the geometry of the flow situation and introduces the relevant variables and constants. Before proceeding, however, various assumptions have to be made to arrive at a mathematically tractable yet physically meaningful set of equations. We will assume a liquid sheet that is thin compared to its horizontal extent. In addition, we will take the fluid flow as laminar and two-dimensional. The pressure in the air cushion does not vary in space, and the air cushion compresses adiabatically and reversibly. Furthermore, the pressure difference across the curtain is much smaller than the atmospheric pressure. Viscous and surface tension effects will be neglected in the analysis, as will the effects of splashing and waves in the lower

basin. Finally, the inlet conditions are not affected by the oscillations of the liquid sheet.

Following a derivation similar to Sundström *et al.*, Weinstein *et al.* (1997) or Mehring & Sirignano (1999), the system of equations governing the liquid sheet can be written as

$$\frac{\partial u}{\partial t} + u\frac{\partial u}{\partial x} = -\frac{p}{\rho h}\frac{\partial f}{\partial x} + g, \quad \frac{\partial v}{\partial t} + u\frac{\partial v}{\partial x} = \frac{p}{\rho h}, \tag{2.1a,b}$$

$$\frac{\partial h}{\partial t} + \frac{\partial (hu)}{\partial x} = 0, \quad \frac{\partial f}{\partial t} + u\frac{\partial f}{\partial x} = v, \tag{2.1c,d}$$

with u and v the fluid velocity in the (downward) x-direction and the (horizontal) y-direction, respectively. The thickness of the liquid curtain is denoted h, the horizontal displacement from the x-axis is denoted f. The variable p stands for the pressure in the liquid sheet, and the acceleration due to gravity is g. In the above equations, only first-order sheet deflections are taken into account.

To close the system we need an expression for the pressure in terms of the dynamic variables (u, v, h, f). Assuming isentropic conditions for the pressure in the cushion we obtain (for an ideal gas)

$$p = p_1 - p_0 = p_0 \left[\left(1 + \frac{1}{LB} \int_0^L f(x)\,\mathrm{d}x \right)^{-\gamma} - 1 \right] \approx -\frac{p_0 \gamma}{LB} \int_0^L f(x)\,\mathrm{d}x, \tag{2.2}$$

where p_1 denotes the pressure in the air cushion, and p_0 the ambient pressure.

We proceed by non-dimensionalizing all velocities by $\sqrt{gL}$, the horizontal displacement of the curtain by a characteristic quantity A, the thickness of the film by the inlet width H, and the pressure by $\rho g H$. The independent variables x and t are scaled by the height L of the curtain and by $\sqrt{L/g}$, respectively. This results in the non-dimensionalized system of equations

$$\frac{\partial u}{\partial t} + u\frac{\partial u}{\partial x} = -\epsilon\frac{p}{h}\frac{\partial f}{\partial x} + 1, \quad \frac{\partial v}{\partial t} + u\frac{\partial v}{\partial x} = \frac{p}{h}, \tag{2.3a,b}$$

$$\frac{\partial h}{\partial t} + \frac{\partial (hu)}{\partial x} = 0, \quad \epsilon\frac{\partial f}{\partial t} + \epsilon u\frac{\partial f}{\partial x} = v, \tag{2.3c,d}$$

$$p = -k \int_0^1 f(x)\,\mathrm{d}x \tag{2.3e}$$

where $\epsilon = A/L$ measures the typical size of horizontal oscillations compared to the length of the curtain, and the parameter $k = \gamma A p_0 / B$ describes the compressibility of the air cushion. Non-dimensionalized boundary conditions of the form

$$u(0,t) = U, \quad h(0,t) = 1, \quad v(0,t) = 0, \quad f(0,t) = 0 \tag{2.4}$$

are imposed at the inlet ($x = 0$).

2.1. *Linearized equations*

Assuming oscillations of the liquid sheet that are small compared to the length of the curtain, we will attempt a regular perturbation approach in the small parameter ϵ with $u = \bar{u}(x) + \epsilon u'(x,t) + O(\epsilon^2)$ for the vertical velocity and accordingly for the other dependent variables.

At $O(1)$ we obtain analytical solutions for the steady velocity, pressure and thickness

profiles as follows:

$$\bar{u}(x) = \sqrt{U^2 + 2x}, \quad \bar{v}(x) = 0, \tag{2.5a,b}$$

$$\bar{p}(x,t) = 0, \quad \bar{h}(x) = \frac{U}{\sqrt{U^2 + 2x}}. \tag{2.5c,d}$$

The next order, $O(\epsilon)$, yields the linear system of equations

$$\frac{\partial u'}{\partial t} + \frac{\partial}{\partial x}(\bar{u}u') = 0, \quad \bar{h}\frac{\partial v'}{\partial t} + U\frac{\partial v'}{\partial x} = p', \tag{2.6a,b}$$

$$\frac{\partial h'}{\partial t} + \frac{\partial}{\partial x}(\bar{h}u' + \bar{u}h') = 0, \quad \frac{\partial \bar{f}}{\partial t} + \bar{u}\frac{\partial \bar{f}}{\partial x} = v' \tag{2.6c,d}$$

$$p' = -\kappa \int_0^1 \bar{f}(x)\,\mathrm{d}x, \tag{2.6e}$$

with $\kappa = p_0\gamma L/B$. The boundary conditions at the inlet are

$$u'(0,t) = 0, \quad v'(0,t) = 0, \quad h'(0,t) = 0, \quad \bar{f}(0,t) = 0. \tag{2.7}$$

This system forms the foundation of the following linear stability analysis.

3. Linear stability analysis

The form of the linear system of equations (2.6) allows the reformulation of the linear stability problem in terms of the horizontal velocity v' and the horizontal displacement $\bar{f}$ from the vertical x-axis only. We obtain

$$\frac{\partial v'}{\partial t} + \bar{u}(x)\frac{\partial v'}{\partial x} = -\kappa\frac{\bar{u}(x)}{U}\int_0^1 \bar{f}(x)\,\mathrm{d}x, \tag{3.1a}$$

$$\frac{\partial \bar{f}}{\partial t} + \bar{u}(x)\frac{\partial \bar{f}}{\partial x} = v'. \tag{3.1b}$$

Using a modal temporal approach we let $\bar{f}(x,t) = F(x)\mathrm{e}^{\mathrm{i}\omega t}$ and $v'(x,t) = V(x)\mathrm{e}^{\mathrm{i}\omega t}$ which upon substitution yields, in matrix form,

$$\begin{pmatrix} -\bar{u}(x)\mathscr{D} & -\kappa\dfrac{\bar{u}(x)}{U}\displaystyle\int_0^1 \mathrm{d}x \\ \mathscr{I} & -\bar{u}(x)\mathscr{D} \end{pmatrix} \begin{pmatrix} V \\ F \end{pmatrix} = \mathrm{i}\omega \begin{pmatrix} V \\ F \end{pmatrix}, \tag{3.2}$$

with $F(0) = V(0) = 0$ as the boundary conditions, $\mathscr{D} \equiv \mathrm{d}/\mathrm{d}x$, and $\mathscr{I}$ as the identity operator.

Equation (3.2) represents the dispersion relation for the liquid curtain in the form of an integro-differential matrix operator. A spectral collocation technique based on Chebyshev polynomials is employed to solve for the eigenvalues; both differentiation and integration are spectrally accurate. Typical values for the compressibility coefficient range from $\kappa = 7 \times 10^3$ to 6×10^4 under laboratory conditions (see table 1 for typical dimensions); the velocity falls within the range of $U = 0.3$ to 1.5. For naturally occurring waterfalls, we typically obtain $\kappa \approx 1000$ and $U \approx 0.1$. The spectrum displayed in figure 2 for $\kappa = 5 \times 10^4$ and $U = 0.4$ shows an eigenvalue distribution that is symmetric about the imaginary axis. For higher phase velocities ω_r, the growth rate ω_i increases until unstable modes are encountered (not shown in figure 2). For even larger phase velocities, negative growth rates prevail again.

Figure 3 depicts the real part of five representative eigenfunctions corresponding to

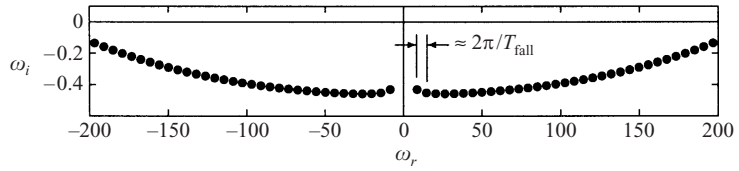

FIGURE 2. Spectrum of a falling liquid sheet for $\kappa = 5 \times 10^4$ and $U = 0.4$.

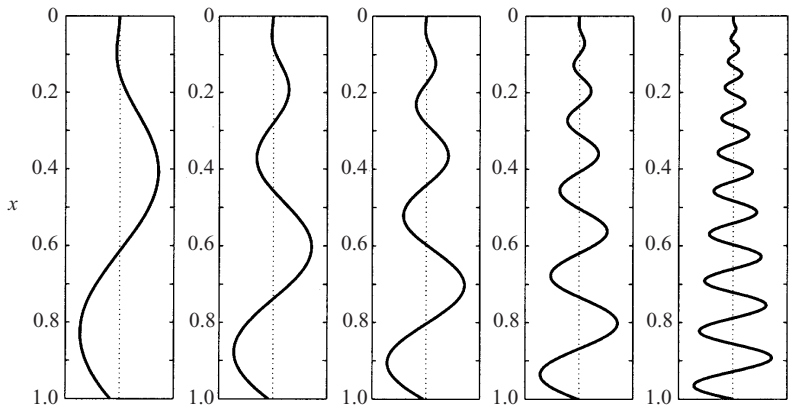

FIGURE 3. Selected eigenfunctions for liquid curtain flow with $\kappa = 5 \times 10^4$ and $U = 0.4$. From left to right: 1st, 2nd, 3rd, 5th and 10th eigenfunction (sorted by ascending positive phase velocity).

the first, second, third, fifth and tenth mode (with an ordering in terms of ascending phase velocity ω_r). These eigenfunctions illustrate the fundamental shapes of the sheet oscillations. Different values of κ and U result in qualitatively similar spectra and eigenfunctions. As is apparent from the eigenfunctions, we have to question the validity of higher-frequency modes in the light of the assumptions we made in the derivation of the governing equations. Viscous and surface tension effects will certainly play a role for these modes. Nevertheless, the low-frequency eigensolutions will be sufficient to explain the overall dynamics of the liquid curtain oscillations, as shown below.

3.1. *Comparison with experiments*

As mentioned in the introduction, experimental efforts have consistently and reliably observed a dominant low-frequency signal that corresponds closely to the fall time $T_{\text{fall}} = \sqrt{U^2 + 2} - U$ of the curtain. In our case we will compare the results of the linear stability analysis with experiments performed by Sundström *et al.* and Baille (1994). The data are given in table 1. The column labelled $f T_{\text{fall}}$ contains the product of measured frequency and fall time, appropriately non-dimensionalized. Throughout the various experiments, this product represents a robust feature of the oscillating liquid sheets that cannot be attributed to the least-stable frequency resulting from a linear stability calculation. It is worth mentioning that even the product of the lowest frequency (based on a linear stability analysis) and the fall time exceeds the measured product by more than 40% for the experimental configurations given in table 1.

3.2. *Multimodal analysis*

We re-examine the behaviour of the linear system by constructing and evolving initial conditions that consist of linear combinations of low-frequency modes. Optimizing

Initial thickness H (mm)	Width B (cm)	Length L (cm)	Initial speed u_0 (m s^{-1})	Observed frequency f (Hz)	$f T_{\text{fall}}$
1.5	17.5	31	2.6	9.85	0.9876
			2.2	9.00	1.0136
			2.4	9.38	0.9956
		39	2.6	8.50	1.0365
			2.4	7.87	1.0126
			2.1	7.50	1.0497
		50	2.6	6.63	0.9939
			2.2	6.00	0.9954
			2.1	5.90	1.0049
2	13.5	70	1.57	4.000	1.0009
			1.70	4.125	0.9996
			1.83	4.375	1.0271
			1.97	4.750	1.0783
			2.10	4.625	1.0181
			2.23	4.875	1.0412
			2.36	5.250	1.0883

TABLE 1. Experimental data for water curtain flow. From Sundström *et al.* and Baille (1994).

this linear combination of eigenfunctions, we hope to recover a frequency feature that not only matches the experimental data, but also displays the same robustness throughout a large parameter range.

Before starting this multimodal analysis we need to derive a physically meaningful way of measuring the size of the perturbation. We decided on the sum of kinetic energy in the horizonal (x) direction and the compression work the curtain performs on the air cushion:

$$E(t) = \underbrace{\frac{1}{2}\int_0^1 |v'|^2 \,\mathrm{d}x}_{\text{kinetic energy}} + \underbrace{\frac{1}{2}\kappa \int_0^1 |\bar{f}|^2 \,\mathrm{d}x}_{\text{compression work}}. \tag{3.3}$$

Based on this disturbance measure we consider initial perturbations that consist of a linear combination of the first $2N$ eigenfunctions obtained from (3.2), i.e.

$$\begin{pmatrix} v' \\ \bar{f} \end{pmatrix} = \sum_{|i|=1}^{N} \alpha_i(t) \begin{pmatrix} V \\ F \end{pmatrix}_i. \tag{3.4}$$

Computing the total energy at time t as a maximum over all possible initial conditions requires the numerical evaluation of (see Schmid & Henningson 2001 for details)

$$\max_{\alpha_i} \frac{E(t)}{E(0)} = \|\boldsymbol{Q} \exp(\mathrm{i}\boldsymbol{\Omega} t)\boldsymbol{Q}^{-1}\|^2 \equiv G(t), \tag{3.5}$$

with $\boldsymbol{Q}^H\boldsymbol{Q} = \boldsymbol{M}$ and the entries of the matrix $\boldsymbol{M}$ given as

$$M_{ij} = \frac{1}{2}\int_0^1 V_i^* V_j + \kappa F_i^* F_j \,\mathrm{d}x. \tag{3.6}$$

The diagonal $2N \times 2N$ matrix $\boldsymbol{\Omega}$ contains the eigenvalues. The maximum amplification of energy (as defined in (3.5)) versus time is plotted in figure 4(a) for the parameter

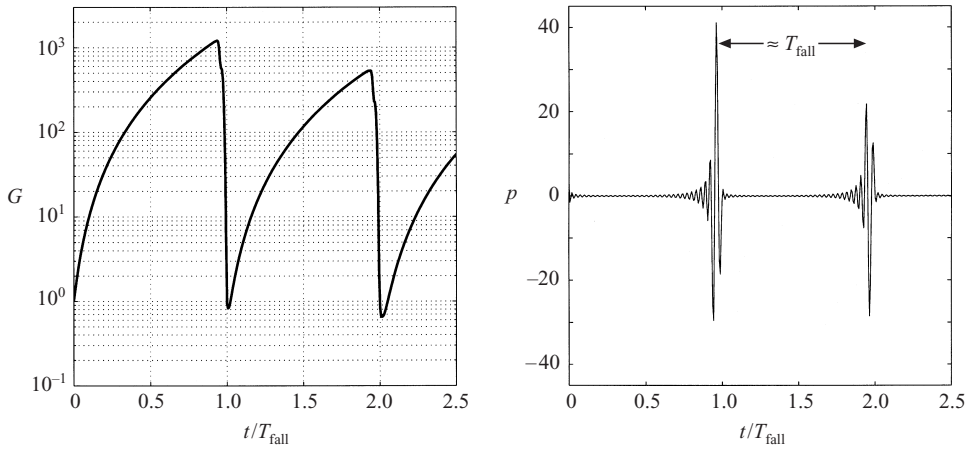

FIGURE 4. Multimodal stability analysis of a falling liquid sheet for $\kappa = 5 \times 10^4$ and $U = 0.4$. (*a*) optimal energy amplification $G(t)$ versus time, see equation (3.5); (*b*) pressure difference p versus time, obtained from the linear evolution of the optimized initial condition.

setting of figure 2. The first $N = 44$ eigenfunctions – spanning a phase velocity range from $\omega_r = -193.08$ to $\omega_r = 193.08$ – have been included in the computations. The time axis is scaled by the fall time $T_{\text{fall}} = \sqrt{U^2 + 2} - U$. We observe the strongest amplification of total energy close to the fall time T_{fall} of the system – in accordance with experimental results. A T_{fall}-periodic pattern is observed that results in a significant amplification of initial energy. Varying the governing parameters, κ and U, produces qualititatively similar results, i.e. strong energy amplification in the form of a T_{fall}-periodic signal. The same is observed when including more (high-frequency) eigenfunctions in the computations. Starting with the optimal linear combination of low-frequency modes we evolve this initial condition according to the linearized equations and compute the difference between the pressure in the air cushion and the ambient pressure as a function of time. The result is plotted in figure 4(*b*). Again, we observe strong pressure peaks whose frequency strongly correlates with the fall time T_{fall}. This is in excellent agreement with experimental data and establishes the T_{fall}-periodic pressure signature of oscillating liquid curtains as a multimodal rather than a modal phenomenon.

The temporal evolution of the curtain shape starting with the optimal initial condition is shown in figure 5. Various interesting features are worth pointing out. Although high-frequency oscillations are present in the liquid sheet, the main deformation of the curtain – and thus the highest amplitude of the pressure in the air cushion – is caused by a wave packet travelling down the sheet. As this wave packet approaches the bottom basin, we notice a deformation of the liquid sheet along its entire length (see the arrow in figure 5) which triggers and gives rise to the formation of a new wave packet near the top of the curtain, hence completing the cycle of T_{fall}-periodic curtain oscillations. The repeated triggering of wave packets running down the curtain is due to the global coupling by the compressible air cushion. In the absence of this coupling, the governing equations reduce to simple advection equations, and once an initial disturbance reaches the lower basin, the oscillatory motion of the liquid sheet terminates. The multimodal analysis also demonstrates that neither a purely sinusoidal pressure oscillation is justified nor a resonance condition has to be invoked

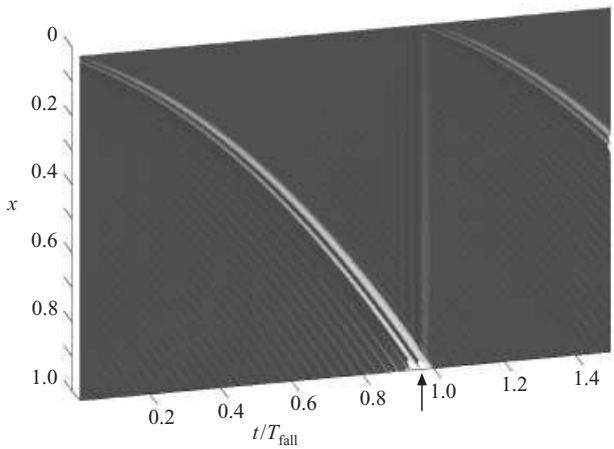

FIGURE 5. Curtain shape versus time for $\kappa = 5 \times 10^4$ and $U = 0.4$ starting with the optimal initial condition, i.e. the initial condition that results in the maximum energy amplification near $t = T_{\text{fall}}$ in figure 4(*a*).

(Treiber 1974) to determine the characteristic frequency of the pressure oscillations in the air cushion.

An alternative explanation of the behaviour shown in figure 5 invokes the concept of global modes. Linear stability theory produces these global modes (see figure 3) that have support over the entire computational domain. A superposition of these global modes can then be used to describe localized structures in the flow, such as wave packets. Cossu & Chomaz (1997) were the first to demonstrate that a superposition of global modes can describe convective propagation of wave packets in a non-parallel flow. Their analysis focuses on the Ginzburg–Landau equation with spatially varying coefficients as a model for many fluid systems. Similarly, in our case, the dynamics of the curtain is not governed by individual global modes but rather by a linear combination of them. The observed frequency signature can therefore not be retrieved from analysing the phase velocities of global modes, but is instead governed by the phase velocity *difference* of a linear combination of global modes. A careful analysis of the spectrum confirms that the real parts ω_r of two consecutive eigenvalues are separated by approximately $2\pi/T_{\text{fall}}$.

The behaviour of the falling liquid curtain is reminiscent of the stability properties of subcritical wakes behind bluff bodies. Although the wake flow is globally stable, a marked response to external forcing as well as large amplification of localized initial conditions are observed (Huerre & Monkewitz 1990). For spatially varying flows a large body of literature (see Huerre & Monkewitz 1990; Huerre 2000 and references therein) addresses the link between global instabilities and local stability characteristics. Monkewitz, Huerre & Chomaz (1987) and Chomaz, Huerre & Redekopp (1991) have proposed a model for the near wake of two-dimensional bluff bodies and, using multiple scales, have derived an expression for the slowly varying amplitude of the dominant global mode. This type of analysis is related more to the approach used by Treiber (1974) than the one taken here, since it describes the frequency selection in the wake by a resonant driving of the slightly damped dominant global mode. A detailed investigation of the link between local and global stability properties for the falling liquid sheet is beyond the scope of this presentation, but is certainly a worthwhile topic for future work.

4. Summary

A stability analysis of a falling liquid sheet enclosing an air cushion has been performed and compared to experimental data. Single mode analysis based on the least-stable or the lowest-frequency global mode has not been successful in reproducing experimental results. However, an approach based on the optimal superposition of many global modes has produced very good agreement with the experimentally observed frequencies. The resulting pressure signal in the air cushion shows a strong correlation with the fall time of particles in the sheet. This correlation can be observed over a wide range of the governing parameters, again in accordance with experimental findings.

We wish to acknowledge Emmanuel de Langre (LadHyX, École Polytechnique), Fritz Bark (Mechanics, KTH Stockholm) and Peter Blossey (University of Washington) for helpful comments and discussions. During the early part of this project, Lars-Göran Sundström (KTH) generously shared his insight into the water curtain problem with us; we were deeply saddened by his untimely death.

REFERENCES

Baille, C. 1994 Rideau d'eau oscillant. *Tech. Rep.* Department of Mechanics, Royal Institute of Technology; also Projet de fin d'etudes, Institut National des Sciences Appliquées, Lyon.

Carman, A. 1960 Report on vibrating nappe. *Tech. Rep.* Dept. Civil Engng, Univ. Witwatersrand, Johannisburg.

Casperson, L. W. 1993 Fluttering fountains. *J. Sound Vib.* **162**, 251–262.

Chomaz, J.-M., Huerre, P. & Redekopp, L. G. 1991 The effect of nonlinearity and forcing on global modes. In *New Trends in Nonlinear Dynamics and Pattern-forming Phenomena* (ed. P. Coulet & P. Huerre), pp. 259–274. Plenum.

Cossu, C. & Chomaz, J.-M. 1997 Global measures of local convective instabilities. *Phys. Rev. Lett.* **78**, 4387–4390.

Cremer, L. & Ising, H. 1972 Selbsterregte Schwingungen von Überfallstrahlen. *Acustica* **27**, 94–107.

Falvey, H. T. 1980 Bureau of reclamation experience with flow-induced vibrations. In *Practical Experiences with Flow-induced Vibrations* (ed. E. Naudascher & D. Rockwell). Springer.

Huerre, P. 2000 Open shear flow instabilities. In *Developments in Fluid Mechanics: A Collective Introduction to Current Research* (ed. G. K. Batchelor, H. K. Moffatt & M. G. Worster). Cambridge University Press.

Huerre, P. & Monkewitz, P. A. 1990 Local and global instabilities in spatially developing flows. *Annu. Rev. Fluid Mech.* **22**, 473–537.

Kemp, A. R. & Pullen, R. A. 1961 Report on the vibrating nappe phenomenon. *Tech. Rep.* Dept. Civil Engng, Univ. Witwatersrand, Johannesburg.

Mehring, C. & Sirignano, W. A. 1999 Nonlinear capillary wave distortion and disintegration of thin planar liquid sheets. *J. Fluid Mech.* **388**, 69–113.

Monkewitz, P. A., Huerre, P. & Chomaz, J.-M. 1987 Preferred modes in jets and global instabilities. *Bull. Am. Phys. Soc.* **32**, 2051.

Naudascher, E. & Rockwell, D. 1994 *Flow-induced Vibrations. An Engineering Guide.* A. A. Balkema.

Partenscky, H. W. & Khloeung, I. S. 1967 Etude des vibrations des lames déversantes. *Rapport soumis au Conseil Natl de Recherches, Ottawa.*

Plesset, M. S. & Prosperetti, A. 1977 Bubble dynamics and cavitation. *Annu. Rev. Fluid Mech.* **9**, 145–185.

Schmid, P. J. & Henningson, D. S. 2001 *Stability and Transition in Shear Flows.* Springer.

Schwartz, H. I. 1966 Edgetones and nappe oscillation. *J. Acoust. Soc. Am.* **39**, 579–582.

Treiber, B. 1974 Theoretical study of nappe oscillation. In *Flow-induced Structural Vibrations* (ed. E. Naudascher), pp. 34–46, Springer.

Weinstein, S. J., Clarke, A., Moon, A. G., Simister, E. A. 1997 Time-dependent equations governing the shape of a two-dimensional liquid curtain, Part 1: Theory. *Phys. Fluids* **9**, 3625.